

## Co-seismic deformation of the 2010 *M*<sub>w</sub>6.9 Yushu earthquake from InSAR images

Shen Qiang<sup>1</sup>, Qiao Xuejun<sup>1</sup>, Wang Qi<sup>1</sup>, Zhang Jingfa<sup>2</sup>, Tan Kai<sup>1</sup> and Yang Shaomin<sup>1</sup>

<sup>1</sup>*Institute of Seismology, China Earthquake Administration, Wuhan 430071, China*

<sup>2</sup>*Institutes of Crustal Dynamics, China Earthquake Administration, Beijing 100085, China*

**Abstract:** Co-seismic ground-surface deformation of the Yushu earthquake on April 14, 2010 is studied on the basis of interferometry principle by using InSAR images from ALOS PALSAR and ENVISAT ASAR pairs. The observed maximum line-of-sight displacement is 54 cm, which is equivalent to a sinistral strike slip of 180 cm on the surface. The location of macro-epicenter is very close to the epicenter determined by in situ investigation, suggesting that InSAR is an ideal tool for quick identification of the macro-epicenter, and thus for timely disaster assessment after a destructive earthquake.

**Key words:** *M*<sub>w</sub>6.9 Yushu earthquake; InSAR; surface displacement; fault; rupture

### 1 Introduction

A *M*<sub>w</sub>6.9 earthquake occurred at Yushu, Qinghai, China on April 14, 2010; it killed nearly 2700 people and injured over 10000<sup>[1,2]</sup>. Figure 1 shows the locations of the earthquake, and the distribution of faults in the epicentral region.

After an earthquake, it is important to locate the related surface rupture(s) accurately and quickly to facilitate rescue and reconstruction, and for selection of sites for scientific monitoring. A quick method is the InSAR technology, which has been widely used in crustal-deformation measurements for its wide-view field,

high accuracy, and all-weather operation<sup>[3–7]</sup>. In this study, we used this technology by analyzing ALOS PALSAR and ENVISAT ASAR images to investigate the co-seismic deformation fields and surface ruptures associated with the Yushu earthquake. We also compared the inferred location of macro-epicenter with that of in situ measurements.

### 2 Data

Previous studies have shown that pairs of interferometers with relatively short valid perpendicular baselines should be used for the purpose of high accuracy<sup>[9]</sup>. To extract information of the Yushu co-seismic deformation field, we selected two pairs ALOS PALSAR and ENVISAT ASAR<sup>[8]</sup> with parameters shown in table 1. The ENVISAT ASAR pair with shorter baseline and temporal span is better than the ALOS PALSAR pair, but it does not cover the entire area affected by the earthquake. The information from ALOS PALSAR pair with L-band is more affected by errors in baseline and extratDEM<sup>[9]</sup>, due to its longer perpendicular baseline, but less affected by vegetation canopy than ENVISAT ASAR with C-band. In this study, both pairs were

Received:2011-04-23; Accepted:2011-05-27

Corresponding author; Tel: + 86 – 18971407030; E – mail: cl980606@hotmail.com

This work is supported by National Natural Science Foundation of China (41004008); Key Foundation of Institute of Seismology China Earthquake Administration (IS201026019); State Key Laboratory of Cryospheric Sciences, Cold and Arid Regions Environment and Engineering Research Institute, Chinese Academy of Sciences (SKL CS09 – 03); the Foundation of State Key Laboratory of Water Resources and Hydropower Engineering Science, Wuhan University(2009B54); the Foundation of Institute of Seismology China Earthquake Administration (IS200826057); National Key Technology R&D Program of China (2008BAC35B04 – 5)

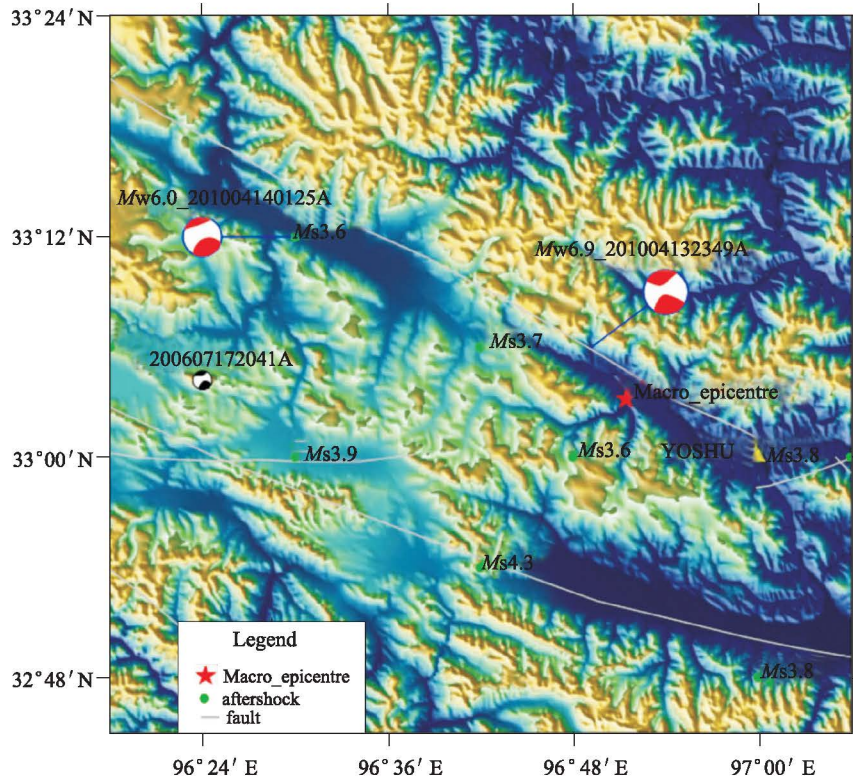


Figure 1 Location of Yushu earthquake and a Mw6.0 aftershock (red balls) and faults (gray lines)

**Table 1 Basic parameters of interferometry**( Here  $B_{\perp}$ ,  $B_x$ ,  $B_y$  represent valid perpendicular, horizontal, and vertical baselines, respectively) (unit:m)

code	sensor	date	$B_{\perp}$	$B_x$	$B_y$
1	ALOS PALSAR	2010 - 01 - 15 - 2010 - 04 - 17	692.7	-840.9	-34.3
2	ENVISAT ASAR	2010 - 02 - 15 - 2010 - 04 - 26	11.9	-35.6	-80.7

used simultaneously in order to validate each other, since no field survey was made while the satellites were overhead. Also, the scope of deformation measurement is larger when both two pairs are used.

### 3 Analysis and results

Figure 2 shows the deformation field derived from ALOS PALSAR measurements together with the locations of Yushu earthquake, a major aftershocks, and faults. The maximum positive and negative line-of-sight (LOS) displacements of 45 cm ( $33^{\circ}3'23.25''N$ ,  $96^{\circ}51'27.00''E$ ) and -54.4 cm, equivalent to nearly 180 cm offset on the surface, are located at  $33^{\circ}4'15.00''N$  and  $96^{\circ}50'14.25''E$ , respectively. The location of the maximum negative displacement is close (370 m) to the location of epicenter ( $33^{\circ}3'11.00''N$ ,  $96^{\circ}51'26.00''E$ ), from in situ investigation, according to the MLR's report (star in Fig. 1). This close agreement

suggests that the InSAR technology is a useful method to quickly determine the macro-epicenter. The location of maximum displacement is about 6 kilometers south-east of the epicenter seismically determined by Harvard university (red ball in Fig. 2), and the difference may be attributed mainly to the aftershock occurrence. Figure 2 shows two other large deformation areas, indicating that the earthquake was associated with at least three surface ruptures. The maximum values of the other two large deformation areas are -20.37 cm ( $33^{\circ}12'53.57''N$ ,  $96^{\circ}28'44.46''E$ ) and -20.25 cm ( $33^{\circ}9'6.33''N$ ,  $96^{\circ}34'34.69''E$ ), respectively (gray diamonds in Fig. 2).

The three ruptures were interpreted on the basis of the InSAR-derived deformation fields. The lengths of the main rupture and the other two ruptures are 35 km, (blue line F1-F1' in Fig. 2), 20 km (F2-F2'), and 8 km (F3-F3'), respectively. The ruptures are nearly parallel to the fault trace at a distance of 1 - 3 km. The



fault is a sinistral strike-slip fault with no obvious vertical displacement, according to seismic fault simulations and field investigation. The result of this study also shows a sinistral strip slip, because the displacements of the southern part are negative (positive represents surface moving toward the satellite along line of sight), meaning an eastward motion, while the northern part shows a westward motion.

Figure 3 shows the LOS displacements along eight profiles (gray lines in Fig. 2) perpendicular to the fault. The largest displacement is as much as 54 cm, which occurred symmetrically within 10 km of the main rupture zone (B1-B1'); the displacements were only 2 cm at distances larger than 10 km from the rupture. This narrowness of deformation zone suggests that the earthquake was mainly associated with surface ruptures having little vertical movement here. Along profiles CC', DD', EE', FF', GG', and HH', the displacements are non-symmetrically distributed, with amplitude 2 to 4 times larger in the southern part than in the northern part. This asymmetry may be due to the

occurrence of aftershocks which were located mainly in the southern part (see black dots in Fig. 2). Except the profiles of DD' and HH', the curves in this figure are nearly vertical at the ruptures, indicating that the results from InSAR can reflect correctly the characteristics of surface deformation near surface ruptures. The non-vertical shape of profiles at the offsets of DD' and HH' maybe related to the fact that the earthquake did not cause any large-scale ruptures on the surface.

The LOS displacement field from ENVISAT ASAR is shown in figure 4. The maximum displacements of  $-15.9$  cm and  $-11.1$  cm shown as black diamonds in the figure are located at  $(96^{\circ}35'46.5''\text{E}, 33^{\circ}9'28.5''\text{N})$  and  $(96^{\circ}26'12.53''\text{E}, 33^{\circ}13'21.37''\text{N})$ , respectively; these are about 2 km and 4 km from the corresponding locations obtained from ALOS PALSAR. Also, both displacement fields from ALOS PALSAR and ENVISAT ASAR are quite similar; the small differences being caused by different geometry of spacecraft platforms. Their accuracies can be evaluated by some in situ measurements, if necessary. Taking all

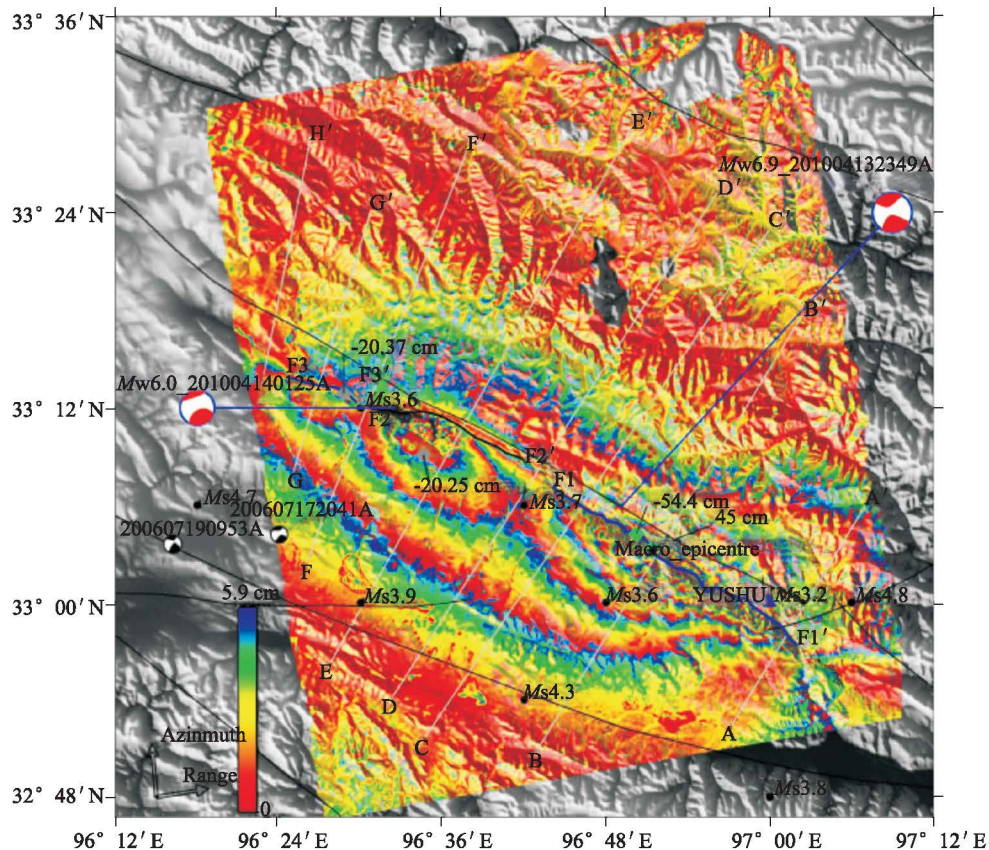


Figure 2 Co-seismic surface deformation of Yushu earthquake from ALOS PALSAR. The gray lines represent the locations where displacement profiles in figure 3 have been extracted; the black solid lines indicate faults; the diamonds show where the maximum displacements occurred

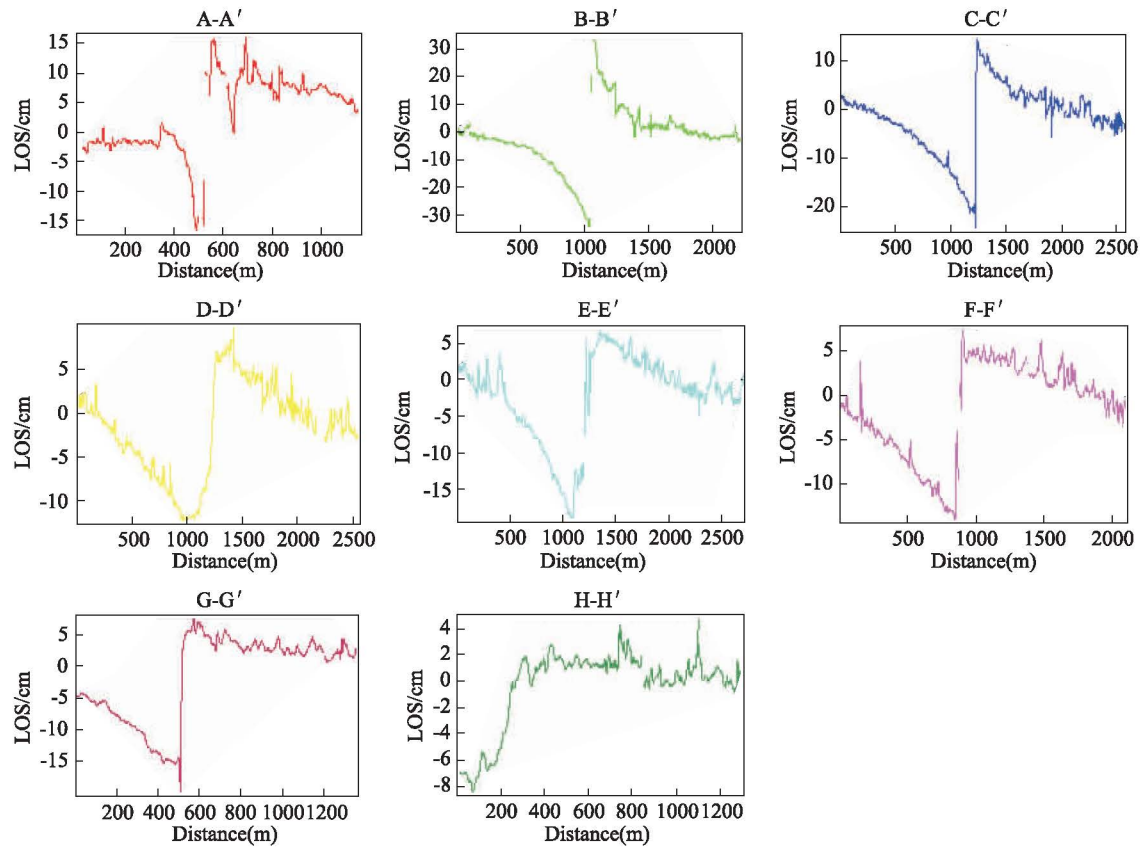


Figure 3 LOS displacements along the profiles

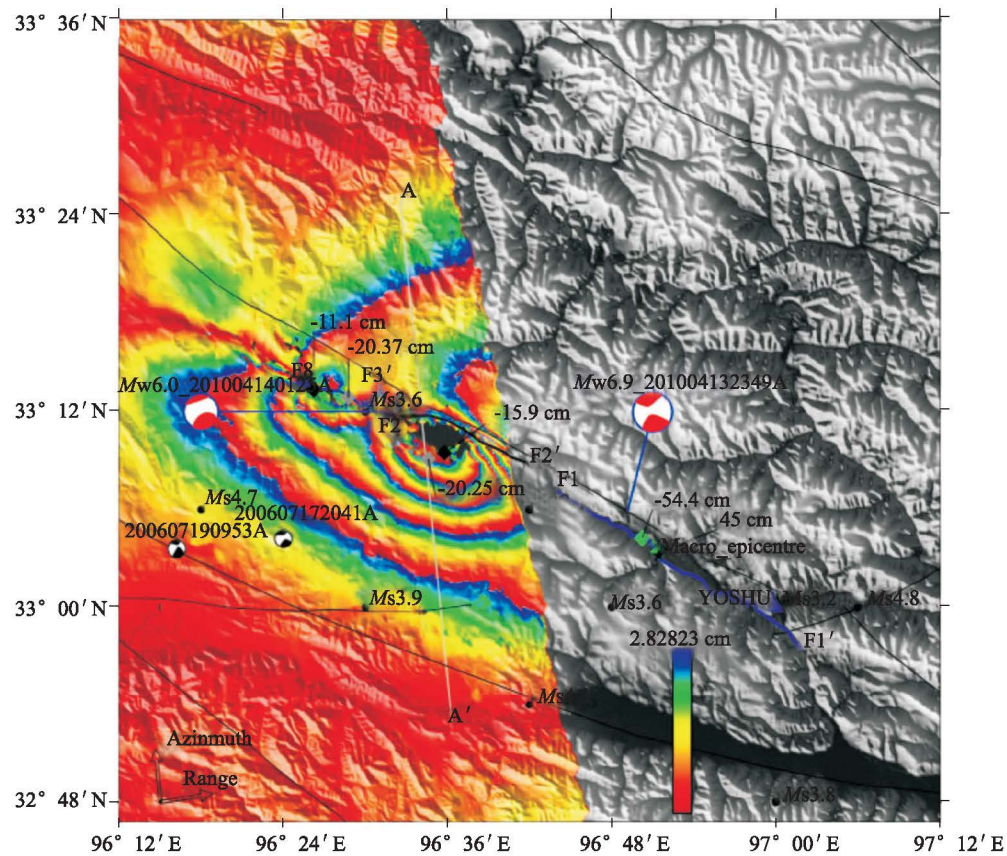


Figure 4 Co-seismic surface deformation of Yushu earthquake from ENVISAT ASAR

the above results into consideration, we think InSAR is an ideal tool for the very important task of identifying the location of macro-epicenter in the efforts of disaster assessment and reconstruction after an earthquake.

## 4 Conclusions

The surface-displacement field associated with the *Mw*6.9 Yushu earthquake has been studied quickly with InSAR technology. The results obtained by simultaneously using images from ALOS PALSAR and ENVISAT ASAR pairs are consistent with each other. The observed maximum displacement is as much as 1.8 m on the ground surface, with the displacements in the southern part generally larger than those in the northern part. The macro-epicenter derived from InSAR is consistent with that obtained from in situ surveys.

## Acknowledgements

We thank JAXA and ESA for providing ALOS PALSAR and ENVISAT ASAR images, respectively.

## References

- [1] <http://www.globalcmt.org/CMTsearch.html>.
- [2] Institute of geophysics, CEA. Preliminary study of 2010 *Ms*7.0 earthquake in Qinghai[R]. Beijing: Institute of geophysics, CEA, 2010 (in Chinese).
- [3] Massonnet D, Rossi M, Carmona C, et al. The displacement field of the Landers earthquake mapped by radar interferometry. *Nature*, 1993, 364:138 – 142.
- [4] Klees R and Massonnet D. Deformation measurement using SAR interferometry: Potential and limitations. *Geologie en Mijnbouw*, 1998, 77(2):161 – 176.
- [5] Qiao Xuejun, You Xinzhaoh, Yang Shaomin, et al. Study on dislocation inversion of *Ms*6.6 Damxung earthquake as constrained by InSAR measurement. *Journal of Geodesy and Geodynamics*, 2009, 29(6):1 – 7. (in Chinese)
- [6] Tan Kai, Shen Qiang, Qiao Xuejun, et al. Test of InSAR coseismic deformation field of Wenchuan *Mw*7.9 earthquake. *Journal of Geodesy and Geodynamics*, 2010, 30(2):14 – 18. (in Chinese)
- [7] Zheng Kang Shen, Jianbao Sun, Peizhen Zhang, et al. Slip maxima at fault junctions and rupturing of barriers during the 2008 Wenchuan earthquake. *Nature Geoscience*, 2009, 2:718 – 724.
- [8] Shu Ning. Principles of radar interferometry. Wuhan: Wuhan University Press, 2003. (in Chinese)
- [9] Li Zhenhong, Liu Jingnan and Xu Caijun. Error analysis in InSAR data processing. *Geomatics and Information Science of Wuhan University*, 2004, 29(1):72 – 76. (in Chinese)
- [10] [http://www.mlr.gov.cn/xwdt/jrxw/201004/t20100421\\_146223.htm](http://www.mlr.gov.cn/xwdt/jrxw/201004/t20100421_146223.htm).